Electrical Engineering in Japan, Vol. 199, No. 4, 2017
Translated from Denki Gakkai Ronbunshi, Vol. 136-B, No. 4, April 2016, pp. 439–446

Positive Creeping Discharge along Aerial Insulated Wire Generated by Lightning Stroke

TOSHIYUKI NISHI,[1] RYOICHI HANAOKA,[2] FRI MURDIYA,[2,3] and KATSUNORI MIYAGI[2]
[1]National Institute of Technology, Toyama College, Japan
[2]Kanazawa Institute of Technology, Japan
3 Riau University, Indonesia

SUMMARY

There are two causes, inductive lightning surge and direct lightning stroke, as the aerial insulated wire accidents accompanying lightning in a power distribution system. When the overvoltage due to the inductive lightning surge invades to the wire core, the creeping discharge can develop along the wire surface from the free end of the binding wire just after a flashover of the post insulator at the wire supporting point. This creeping discharge may give rise to the accidents such as a melting or snapping of the wire. The creeping discharge along the wire surface has the positive or negative polarity. Positive creeping discharge is restricted to the area where a positive lightning generates. Only a few examples have been reported on the positive creeping discharge, and its characteristic has many unsolved points. In the previous studies, we have observed the positive creeping discharges along the wire surface under the negative inductive lightning surge with the peak values in the range $|V_m| \leq 80$ kV. In this study, the positive creeping discharges are examined newly in the range $|V_m| > 80$ kV. It is reported that the positive creeping discharges are greatly affected by the negative corona discharges generating from the wire surface in $|V_m| \geq 95$ kV. © 2017 Wiley Periodicals, Inc. Electr Eng Jpn, 199(4): 13–21, 2017; Published online in Wiley Online Library (wileyonlinelibrary.com). DOI 10.1002/eej.22947

Keywords: aerial insulated wire; positive creeping discharge; inductive lightning surge; standard lightning impulse.

1. Introduction

High-voltage aerial insulated wires in urban areas are fixed to pole insulators with binding wires. Most accidents on insulated lines are caused by lightning [1], which is briefly categorized into inductive lightning strokes and direct lightning strokes. Line accidents caused by inductive lighting surges have been sharply reduced due to protection measures developed through long-time research [2]. However, despite fewer accidents caused by inductive lightning strokes, invasion of inductive lighting surges to core conductor still remains a problem. In addition, when inductive lighting surge results in flashover on the insulator surface where wire is supported, creeping discharge develops on the wire surface from the tip of binding wire, but no protection measures have been yet established in this regard. Thus, creeping discharge due to inductive lightning strokes remains a cause of wire insulation punctures and other accidents. Therefore, protection measures against inductive lightning strokes and clarification of characteristics of creeping discharge are still important issues.

The surface of electric wires laid outdoors may involve spots where insulation performance is impaired due to blemishes rain, snow, temperature swing, and other natural conditions. When creeping discharge reaches such weak spots on wire surface, punctures are very likely to occur, but discharge may also pass through without punctures. In the latter case, creeping discharge quickly extinct naturally. However, repeated development of creeping discharge puts electric stress on the wire coating. As a result, coating puncture may eventually occur when creeping discharge repeatedly reaches a weak spot on wire surface. If weak spots locate beyond the reach of creeping discharge, they can be excluded from accident factors. Therefore, determination of maximum length of creeping discharge caused by inductive lightning would enable to define critical range of weak spots on wire surface as well as insulation reinforcement range near a wire support point.

There are many factors affecting creeping discharge on wire surface, such as peak value and wavefront length

of inductive lightning surge as well as wire surface conditions. Moreover, these factors complexly affect on each other, which complicates the clarification of creeping discharge characteristics. Previously, we observed creep discharge on wire surface caused by inductive lightning under various conditions, and clarified discharge characteristics heavily depending on different factors [3–13]. On the other hand, occurrence timing and development characteristics of lightning-induced creeping discharge vary with discharge polarity, which requires further clarification.

Polarity of creeping discharge depends on that of cloud-to-ground discharge. In the case of summer lightning, cloud-to-ground discharge is mostly negative. Negative winter lightnings also form, and therefore inductive lightning surges are often positive. As a result, creeping discharge developing on wire surface due to inductive lightning surge is often negative, irrespective of location or season. On the other hand, positive cloud-to-ground discharge is observed with winter lightnings in Hokuriku Region in Japan. In this case, inductive lightning surge is negative, and creeping discharge developing on wire surface becomes positive. Creeping discharges of positive polarity are often observed at locations where positive lightnings occur, but their frequency is lower as compared to the negative creeping discharge. Hence, observation examples are limited, and many points remain unclear.

In our previous work [8], we thoroughly examined the positive creeping discharge developing on wire surface caused by inductive lightning surge, and proposed a discharge development model based on the observed characteristics. Negative impulse voltage simulating negative inductive lightning surge is used to reproduce positive creeping discharge in laboratory (details are given in Section 2). In this study, applied impulse voltage is expressed by peak value $|V_m|$, but this means negative voltage. Electric field on the coating surface of aerial insulated wire grows with peak value increase of inductive lightning surge penetrating to the core conductor. It has already been reported that corona discharge occurs from dielectric surface when electric field on the surface exceeds breakdown strength [14]. Previously, we reported that corona discharge occurs from wire coating surface when inductive lightning charge with high peak value penetrates to the core conductor as assumed in this study [13]. In the case that corona discharge occurs and creeping discharge develops along the dielectric surface, it is predicted that the development of the creeping discharge is affected by the corona discharge. However, there is hardly any observed example of such influence [11].

In the previous studies [3, 8], we observed creeping discharge only at $|V_m| \leq 80$ kV because of laboratory space limitations. However, real inductive lightning surge may have peak value $|V_m| > 80$ kV [1], where the development characteristics of positive creeping discharge remained unclear. In this study, we improved laboratory conditions to explore length and other development characteristics of

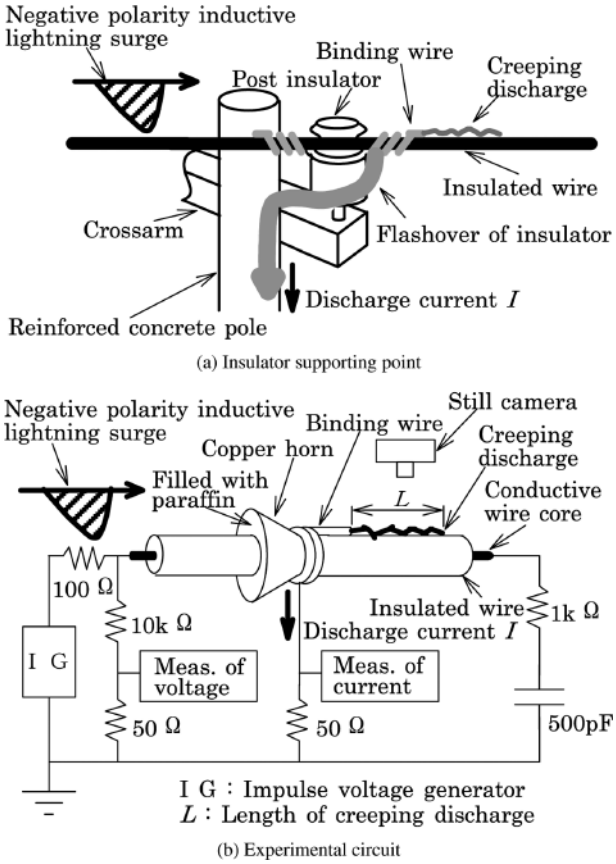

Fig. 1. Schematics of insulator supporting point at reinforced concrete pole and experimental circuit.

positive creeping discharge in the region of $|V_m| > 80$ kV, which was so far unavailable. As a result, different from the previous reports [3, 8], it was observed that negative corona discharge occurs from the wire surface with the increase of $|V_m|$, which strongly influences positive creeping discharge. This special phenomenon is reported here.

2. Experimental Methods

The support portion of utility pole and its experimental circuit are shown schematically in Fig. 1. In the figure, impulse voltage generator (IG) generates standard lightning impulse voltage ($|V_m| = 85$ kV to 100 kV, negative polarity, wavefront length 1.2 μs, and wavetail length 50 μs), and this voltage was applied just once to core conductor as negative inductive lightning surge. In this case, we observed development length and conditions of creeping discharge from the binding wire tip by means of a still camera equipped with an image intensifier. Normally, creeping discharge occurs from both ends of the binding wire when impulse voltage is applied to core conductor, but in this experiment, we made arrangements so that discharge occurs only from

Table 1. Data of insulated wire

Finished outside diameter (mm)	Conductor: Stated cross-section (mm²)	Conductor: Structure (wires/mm)	Conductor: Outside diameter (mm)
10.0	22	7/2.0	6.0
	Insulation		
Thickness of insulated material (mm)	Main material		Relative dielectric constant
2.0	Polyethylene		2.3

one end for easier observation. Specifically, a copper horn was attached to one end of the binding wire as shown in Fig. 1, and paraffin is filled between the wire and the horn to shield the wire. In addition, assuming flashover occurs on the insulator surface, the binding wire was grounded through a discharge current detection resistance (50 Ω). Thus, the binding wire was used only as an electrode for creeping discharge development, and its edges were fixed so as to slightly touch the insulated wire surface. The binding wire was an alloy wire (lead: 97% and antimony: 3%) with straight-cut edges.

Specifications of the insulated wire used in experiment are given in Table 1. This is a 6600-V class 5-m long polyethylene insulated wire mounted at 75 cm above the floor for easy observation. A grounded copper plate was placed on the laboratory floor, thus simulating the earth surface. After development of creeping discharge, the insulated wire surface was grounded, and residual charge was removed by wiping with alcohol. Besides, the laboratory was air-conditioned to maintain air temperature (around 20 °C) and humidity (around 40%). It should be noted that the voltage applied to the insulated wire and creeping discharge are of the opposite polarity in Fig. 1.

3. Experimental Results and Discussion

3.1 Relationship between peak value of applied voltage and development length of positive creeping discharge

Figure 2 illustrates the relation between $|V_m|$ and development length of positive creeping discharge. Each measuring point in the range of $|V_m| \leq 90$ kV pertains to average of 10 measurements. As regards measuring points at $|V_m| = 95$ kV and 100 kV, two kinds of development lengths were observed (to be explained later), and both

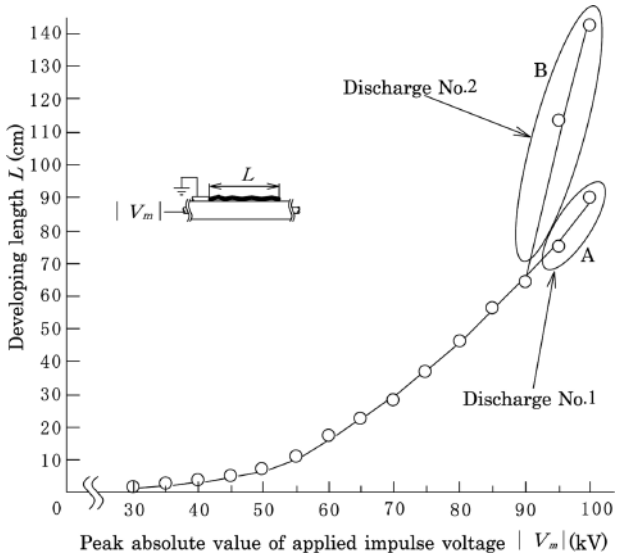

Fig. 2. Relationship between applied impulse voltage and length of positive creeping discharge.

voltage values were observed 100 times to determine occurrence frequency. The discharge length was averaged for the occurrence count of each kind of discharge. Variance in the length data was around ±10% in all cases. The data obtained at $|V_m| \leq 80$ kV were cited from a previous report [3]. As can be seen from the figure, the development length of positive creeping discharge grows monotonely with $|V_m|$ increase within $|V_m| \leq 90$ kV. However, in the range of $|V_m| > 90$ kV, there are two cases (marked by ellipses in Fig. 2): slow growth (A) and fast growth (B). Below, we refer to the former as discharge no. 1, and to the latter as discharge no. 2. In our observations, occurrence frequency of discharge no. 2 was around 17% at $|V_m| =$ 95 kV and around 44% at $|V_m| = 100$ kV. That is, discharge no. 2 occurs more frequently as $|V_m|$ is increased. Discharges no. 1 and no. 2 are defined below in Part (2) of Section 3.5.

3.2 Development of positive creeping discharge

Development of discharges no. 1 and no. 2 from the binding wire tip at $|V_m| = 100$ kV is exhibited in Figs. 3(a) and 3(b). Here, the respective discharge development length is 90.5 cm and 141.2 cm. As can be seen from Fig. 3(a), a leader with strong light emission develops from the wire surface and then branches in the case of discharge no. 1. Similar conditions are always observed at $|V_m| \leq 90$ kV. On the other hand, in the case of discharge no. 2, even stronger light emission is observed in the leader as shown in Fig. 3(b). As reported previously [8], positive creeping discharge develops through ionization caused by collision

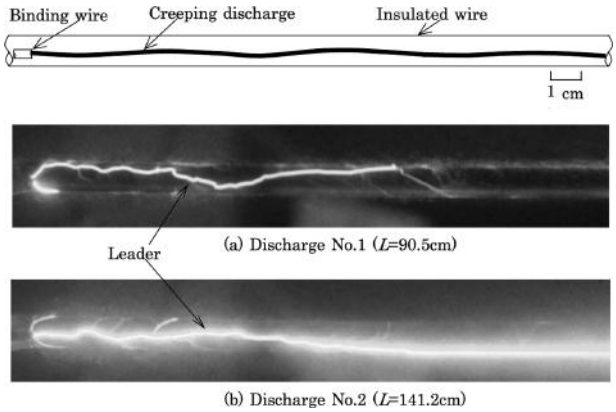

Fig. 3. Typical aspects near binding wire tip at $|V_m| = 100$ kV.

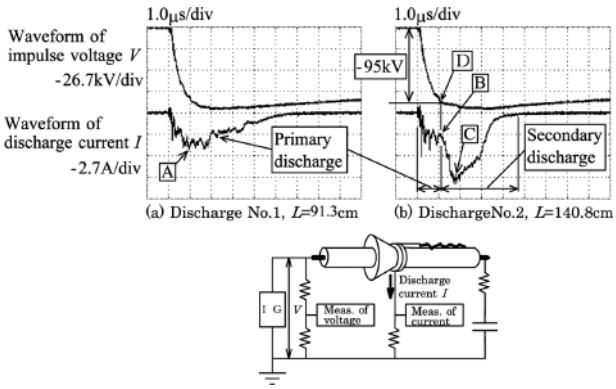

Fig. 4. Waveforms of applied impulse voltage and typical current of positive creeping discharges in discharges no. 1 and no. 2 at $|V_m| = 100$ kV.

with nitrogen molecules as accidental electrons near discharge tip are attracted by positive ions. The difference in light emission strength in Figs. 3(a) and 3(b) can be attributed to the intensity of collision ionization that occurs at the discharge tip.

3.3 Current waveform of positive creeping discharge

Waveforms of the applied voltage and the typical discharge current for discharges no. 1 and no. 2 at $|V_m| =$ 100 kV are shown in Figs. 4(a) and 4(b), respectively. Here, the respective discharge development length is 91.3 cm and 140.8 cm. As shown in Fig. 4(a), the peak value of current in discharge no. 1 is about 4.7 A at point A. On the other hand, the current waveform of discharge no 2 is different from that of discharge no. 1 as can be seen in Fig. 4(b). The current is similar to that of discharge no. 1 in Fig. 4(a) up to point B, after which the current grows sharply to about 9 A (point C) and then decays rapidly. As shown in Fig. 4(b), the core conductor potential at point B is –95 kV (point D). Since discharge no. 2 occurs at $|V_m| \geq$ 95 kV, the core conductor potential upon the sharp growth of current is consistent with the voltage at which discharge begins. This can explain the peculiar phenomenon of sharp growth in current at the applied voltage of –95 kV. It is assumed that the current waveform of discharge no. 2 first appears to be similar as that of discharge no. 1 (referred to as primary current hereafter), and then fast growing current superposes (referred to as secondary current hereafter). Light emission of discharge no. 2 is comparable to that in Fig. 3(a) when primary current flows, while the emission becomes stronger as the one shown in Fig. 3(b) as secondary current begins. In other words, the difference in light emission intensity between Figs. 3(a) and 3(b) is attributed to the difference in collision ionization rate (i.e., the difference between primary and secondary currents).

3.4 Occurrence of negative corona discharge from wire surface

As reported previously [11], the length and the light emission strength of negative creeping discharge occurring on the wire surface when positive inductive lightning surge (V_m) penetrates to the core conductor increase at $V_m \geq$ 90 kV, which is the same as with the positive creeping discharge observed in the present study, and further the discharge current grows as well. This is because when positive impulse voltage applied to the core conductor reaches 90 kV and more, positive corona discharge, which has opposite polarity of that of negative creeping discharge developing on the wire surface, develops from the wire surface to air, thus promoting the development of negative creeping discharge. Similar mechanism might explain the increase in development length, light emission, and discharge current observed in positive creeping discharge at $|V_m| \geq 95$ kV in this study. To confirm this hypothesis, we examined the presence of corona discharge from the wire surface by the experimental circuit shown in Fig. 5. Corona discharge originating from wire surface is very weak. Accordingly, when creeping discharge occurs from binding wire tip, its strong light emission blocks the corona discharge observation. Thus, we ungrounded the binding wire so as to prevent development of creeping discharge. In this state, we applied one-time negative impulse voltage to the core conductor, and observed the wire surface by means of a still camera equipped with an image intensifier.

Figure 6 presents the typical examples of discharge on the wire surface under negative impulse voltage ($|V_m| = 100$ kV) applied to the core conductor. As can be seen from Fig. 6, needle-like corona discharge with a length about 1 cm occurs above and below the wire surface (A, B). Although such corona discharge seems to have occurred

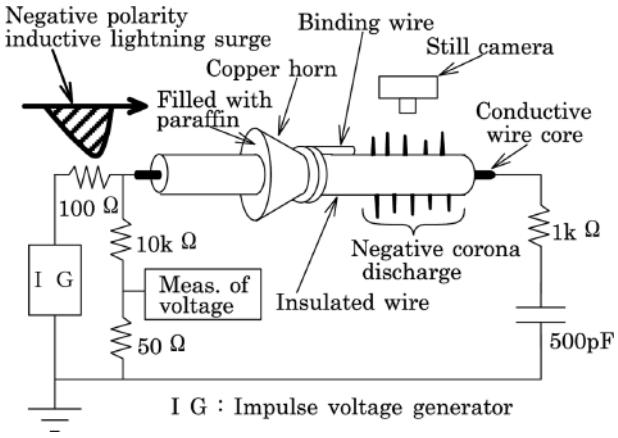

Fig. 5. Experimental circuit for corona discharge observation.

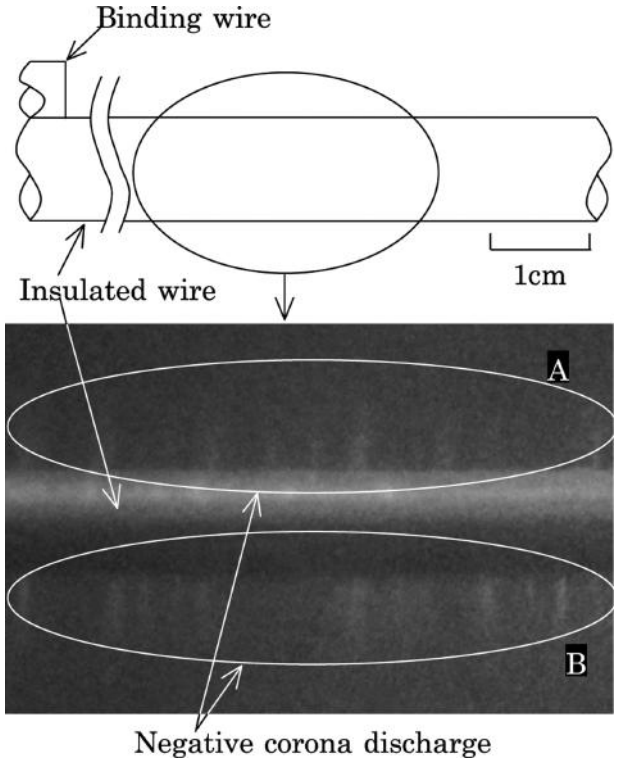

Fig. 6. Typical aspect of negative corona discharge from wire surface at $|V_m| = 100$ kV.

only upward/downward of the wire, observation at varied camera position shows that this corona discharge actually occurs radially around the entire wire surface. Corona discharge occurs due to the increase of negative potential of the core conductor, and therefore it has negative polarity. This negative corona discharge was only observed at $|V_m| \geq 95$ kV. This critical value (–95 kV) agrees with the core conductor potential upon fast growth in discharge current in Fig. 4(b). In order to determine the occurrence frequency of negative corona discharge, we conducted 100 observations at $|V_m| = 95$ kV and 100 kV. The obtained frequency was about 16% and 45%, respectively, which matches very well with the occurrence frequency of discharge no. 2. Thus, it is considered that, when core conductor potential reaches –95 kV and secondary current begins to flow, the corona discharge of negative polarity (opposite to that of creeping discharge) occurs from the wire surface, which promotes the development of positive creeping discharge. This negative corona discharge is likely to be responsible for the sharp growth of discharge current at $|V_m| = 95$ kV as mentioned in Section 3.3.

3.5 Development model

1. ***Negative corona discharge from wire surface.*** Development model of negative corona discharge on wire surface is shown in Figs. 7(a) to 7(d). As shown in Fig. 7(a), when negative impulse voltage of $|V_m| \geq 95$ kV is applied to the core conductor, needle-like negative corona discharge (e.g., A, B) occurs vertically from the wire surface. Initial electrons triggering the negative corona discharge are accidental electrons around the wire. As shown in Fig. 7(b), the electric field on the wire surface grows with the increase of negative potential of the core conductor, and accidental electrons C, D near the wire surface are repulsed and accelerated due to the core conductor potential. These accelerated electrons get involved in collision ionization with nitrogen molecules E in air to generate electrons G and positive ions F, as shown in Fig. 7(c). This phenomenon takes place on the whole wire surface. In this case, electron avalanche occurs at discharge tip, leaving behind slow positive ions, and plasma state H forms on the wire surface, as shown in Fig. 7(d). Since this plasma has high electric conductivity, electrons repulsed by electric field on the wire surface move toward corona discharge tip and concentrate there. As electric field intensifies, electrons I are emitted. At this moment, new electrons and positive ions are generated through collision ionization with nitrogen molecules, and corona discharge develops. On the other hand, many positive ions adhere to the wire coating surface to suppress the wire surface electric field. Moreover, the potential drop occurs inside the corona as discharge develops. As a result, the electric field at the corona discharge tip declines, electron avalanche is inhibited, and corona discharge stops.

2. ***Positive creeping discharge.*** Discharges no. 1 and no. 2 are defined as follows for discussion.

- Discharge no. 1: only primary current occurs

Primary discharge: only collision ionization with accidental electrons at creeping discharge tip is involved.

Primary current: current produced by primary discharge.

- Discharge no. 2: secondary discharge occurs after primary discharge

Secondary discharge: discharge of collision ionization at creeping discharge tip activated by negative corona discharge from wire surface.

Secondary current: current produced by secondary discharge.

Based on the above definitions, we propose a development model for discharge no. 2.

Translation model from primary to secondary discharge at $|V_m| \geq 95$ kV is shown in Figs. 8(a) to 8(d). Development mechanism of the primary discharge at $|V_m| \leq 80$ kV was described in a previous report [8], and only a brief summary is given here. As shown in Fig. 8(a), plasma state A including positive ions and electrons is formed in the leader as positive creeping discharge develops, and positive ions B are generated at the discharge tip due to high electric field. Accidental electrons C at the discharge tip are attracted by these positive ions. Electrons E and positive ions F are produced through collision ionization with nitrogen molecules D during this process. Electrons E are attracted by positive ions B located at the discharge tip, thus continuously forming electron avalanches. Slow positive ions F are left behind, which are attracted by negative potential of the core conductor and aggregate near the wire surface to form new clusters of positive ions. As this process is repeated, positive creeping discharge develops. This is the development process of primary discharge.

As core conductor potential grows and reaches –95 kV, it is considered that secondary discharge occurs through the following process. With the increase of the core conductor potential, accidental electrons G are accelerated near the wire surface, as shown in Fig. 8(b). Electrons G get involved in collision ionization with nitrogen molecules H existing around the wire, thus generating electrons I and positive ions J. After that, negative corona discharge occurs from the wire surface toward ambient air through the process presented in Fig. 7. At this moment, electrons L, M are emitted from plasma portion of negative corona discharge occurring on the wire surface, as shown in Fig. 8(c). On the other hand, high-conductivity plasma state forms in positive creeping discharge, and thus the accidental electrons at the discharge tip as well as electrons generated at the tip of negative corona discharge are attracted by positive ion group Q. In this process, positive ions O and electrons P are newly generated through collision ionization with nitrogen molecules in air. Positive ions O are attracted by negative potential of the core conductor, and adhere to the wire surface, contributing to the development of positive creeping discharge. Electrons P are attracted by the tip of positive creeping discharge, which promotes plasma formation inside the discharge. Accordingly, when negative corona discharge forms from the wire surface, collision ionization is activated near the tip of positive creeping discharge, and discharge development is accelerated, as shown in Fig. 8(d). It is considered that negative corona discharge observed in

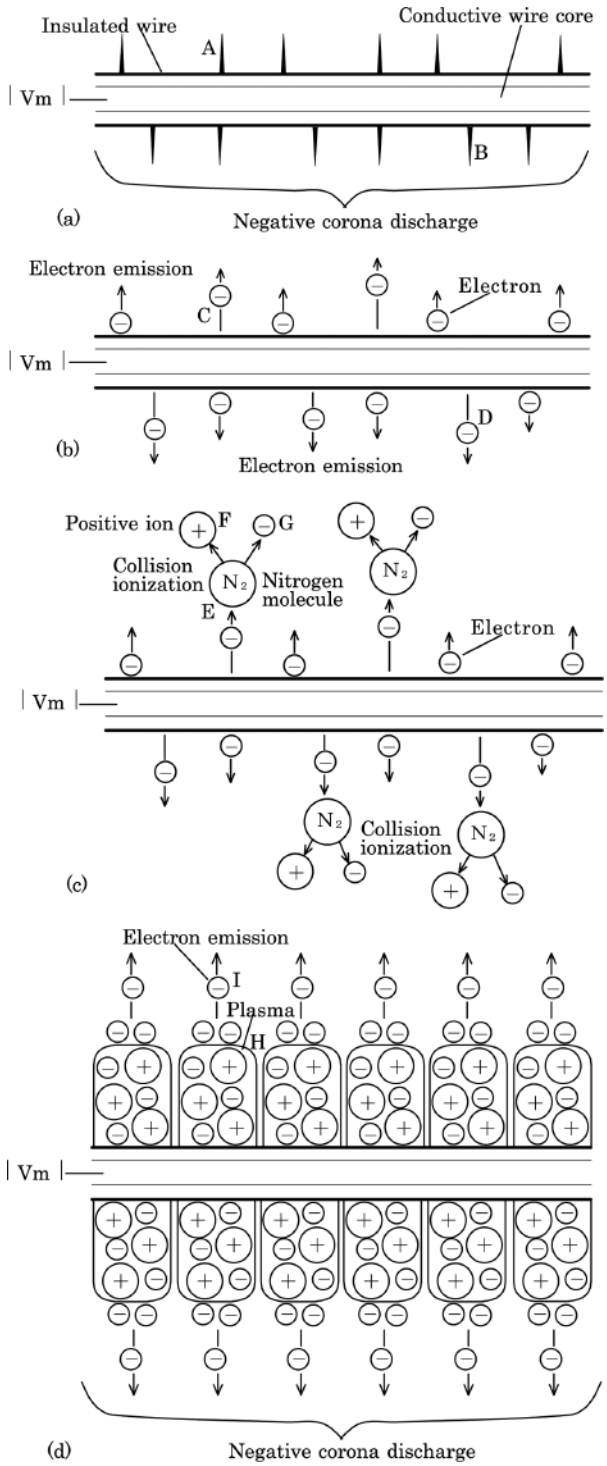

Fig. 7. Developing model of negative corona discharge from wire surface.

this study was formed due to secondary discharge at $|V_m| \geq 95$ kV caused by activation of collusion ionization. As a result, discharge no. 2 shows higher discharge current and stronger leader emission as compared to discharge no. 1 in which only primary discharge occurs.

At $|V_m| \geq 95$ kV, the negative corona discharge originating from the wire surface is supposed to complicate the development characteristics of the positive creeping discharge, and we investigated the development model in this case. This is useful for development of techniques to suppress creeping discharge and for clarifying discharge characteristics.

4. Discussion for Real System

In these experiments, we mounted wire at a height of $h = 75$ cm because of laboratory space limitations and ease of observation. However, the real aerial insulated wires are supported by post insulators at a height about $h = 10$ m. Electric field induced by lightning on wire surface also varies with the wire type and installation height. Negative corona discharge occurs from wire surface as the electric field exceeds a critical level. In these experiments, the peak value of the voltage applied to produce negative corona discharge was $|V_m| = 95$ kV. Therefore, electric field Ew on wire surface at $h = 75$ cm, $|V_m| = 95$ kV is about 36 kV/cm in terms of static field on cylindrical dielectric surface [3]. In other words, this value defines electric field at which negative corona discharge initiates from wire surface.

On the other hand, in a real system, $|V_m| \approx 140$ kV is calculated to achieve the critical field ($E = 36$ kV/cm) on the surface of wire mounted at $h = 10$ m [3]. That is, it is assumed that in a real system, negative corona discharge occurs from wire surface when inductive lightning charge with peak value of $|V_m| = 140$ kV penetrates to the core conductor, which affects positive creeping discharge developing on the wire surface.

5. Conclusion

Winter lightnings in Hokuriku Region facing the Sea of Japan involve positive cloud-to-ground discharges. In this case, inductive lightning surges penetrating to core conductor of aerial insulated wires have negative polarity, and positive creeping discharge occurs on the wire surface in the case of post insulator breakdown. Besides, peak value of inductive lightning surge varies with cloud-to-ground discharge current, distance between lighting stroke point and electric wire, and so on. In this study, we explored development length and current of positive creeping discharge at surge peak voltage $|V_m| > 80$ kV in detail, and discussed discharge development model. The acquired new findings are summarized below.

1. Discharge development length

- When electric field on wire surface originating from inductive lightning surge is $Ew \geq 36$ kV/m

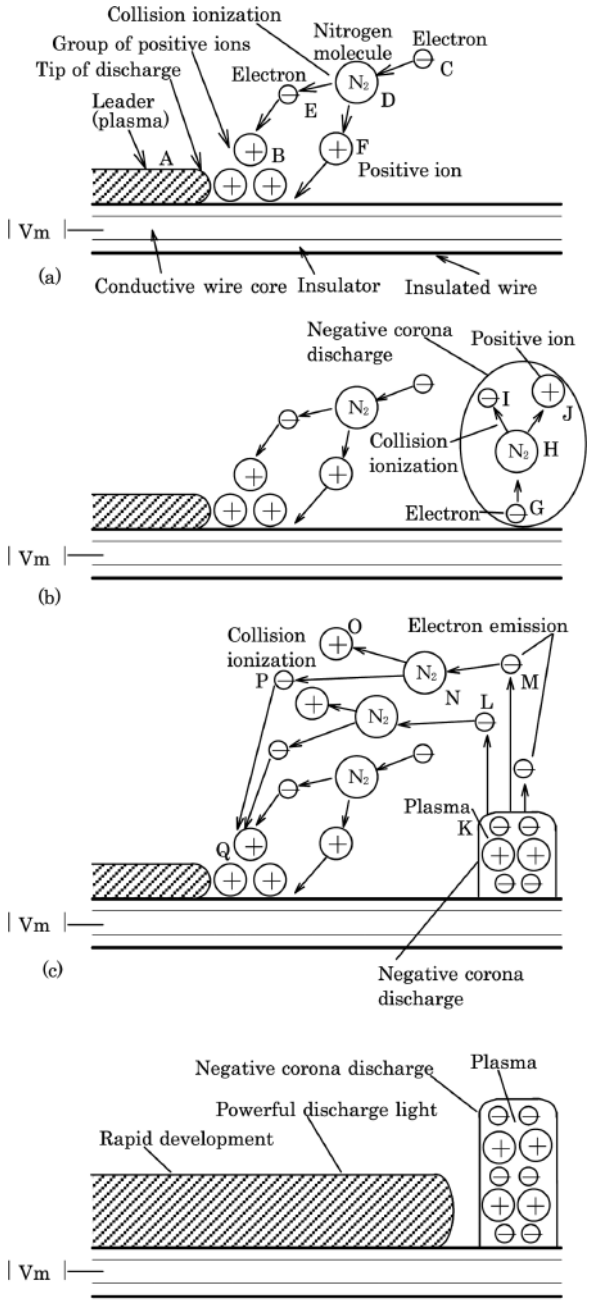

Fig. 8. Translation model of positive creeping discharge from discharge no. 1 to discharge no. 2.

(corresponds to $|V_m| > 95$ kV in this study), there are two cases of discharge development: slow (discharge no. 1) and fast (discharge no. 2).

- Occurrence frequency of discharge no. 2 grows with $|V_m|$ increase.
- The fast growth of discharge length is explained by the fact that negative corona discharge occurs from the wire surface as the potential of the core conductor rises, and this negative corona discharge

promotes the development of positive creeping discharge.

2. Discharge development situations

- Discharge no. 1 develops while branching along the wire surface.
- Discharge no. 2 produces stronger light emission than discharge no. 1. This is because ionization at the tip of positive creeping discharge is activated by the negative corona discharge.
- At $Ew \geq 36$ kV/m, needle-like negative corona discharge with a length about 1 cm occurs from the wire surface vertically toward ambient air.
- Occurrence frequency of negative corona discharge grows with $|V_m|$ increase.

3. Discharge current waveform

- In discharge no. 2, current same as in discharge no. 1 (primary current) flows for about 1 μs until Ew reaches 36 kV/m.
- As Ew reaches 36 kV/m, discharge current nearly doubles rapidly (secondary current). The secondary current occurs because negative corona discharge on the wire surface activates ionization at the tip of creeping discharge.

Positive creeping discharge on wire surface caused by inductive lightning surge is limited to territories where winter lightnings with positive cloud-to-ground discharge occur. Hence, fewer observation examples are available as compared to negative creeping discharge, and many points still remain unclear. In this study, we found that as peak value of inductive lightning surge voltage rises and electric field on wire surface grows, negative corona discharge initiates from the wire surface, which is significantly correlated with the development of positive creeping discharge. Based on this result, we investigated development models for positive creeping discharge accompanied by increase of core conductor potential. These models provide important guideline from the viewpoint of insulation reinforcement at wire support point and prevention of line accidents. In addition, these models can be useful to clarify development mechanisms of similar creeping discharges.

Acknowledgments

We express our gratitude to all those who cooperated in this research.

REFERENCES

1. Electric Technology Research Association. Lightning protection in distribution lines. Electrical Cooperative Research, Vol. 40, 1985. (in Japanese)
2. Investigating R&D Committee on Forecast Technique of Lightning Damage Rate on Power Distribution Lines. Present state and future trends in sparkover probability prediction in distribution lines. IEEJ Tech Rep, No. 937, 2003. (in Japanese)
3. Nishi T, Hanaoka R, Ishibashi R. Impulse creeping discharge phenomena on aerial insulated wire under dry and wet conditions. T IEE Japan 1996;116(4):482–488. (in Japanese)
4. Nishi T, Hanaoka R, Miyamoto T. Influence of applied impulse voltage on creeping discharges along aerial insulated wire. T IEE Japan 1997;117(1):130–136. (in Japanese)
5. Nishi T, Hanaoka R, Miyamoto T. Influence of electric field strength of wire surface on creeping discharges along aerial insulated wire. T IEE Japan 1998;118(1):85–91. (in Japanese)
6. Nishi T, Hanaoka R, Takata S, Miyamoto T. Influence of duration of wave front of impulse voltage on creeping discharges along aerial insulated wire. IEEJ Trans PE 2003;123(1):83–89 (in Japanese); Electrical Engineering in Japan 2004;147(2):30–38 (in English).
7. Nishi T, Hanaoka R, Takata S, Miyamoto T. Characteristics of creeping discharge along aerial insulated wire under impulse voltage with various durations of wave front. IEEJ Trans PE 2005;125(11):1091–1097 (in Japanese); Electrical Engineering in Japan 2007;158(3):29–37 (in English).
8. Nishi T, Hanaoka R, Takata S. Developing process of positive creeping discharge along aerial insulated wire. IEEJ Trans PE 2008;128(9):1111–1118 (in Japanese); Electrical Engineering in Japan 2010;173(3):20–29 (in English).
9. Nishi T, Hanaoka R, Takata S. Developing process of negative creeping discharge along aerial insulated wire. IEEJ Trans PE 2010;130(4):443–450. (in Japanese)
10. Nishi T, Hanaoka R, Takata S. Transition of progressing aspect of negative creeping discharge along aerial insulated cable. IEEJ Trans PE 2011;131(9):786–792. (in Japanese)
11. Mizuno T, Hanaoka R, Nishi T, Takata S, Kanamaru Y. Distinctive discharge generated under impulse voltage and negative creeping discharge along aerial insulated cable. IEEJ Trans FM 2010;130(11):993–998.
12. Nishi T, Hanaoka R, Takata S. Relationship between creeping discharge along aerial insulated wire and duration of wave front of inductive lightning surge. IEEJ Trans PE 2013;133(3):277–285 (in Japanese); Electrical Engineering in Japan 2014;189(1):23–35 (in English).
13. Nishi T, Hanaoka R, Murdiya F, Miyagi K. Negative creeping discharge along aerial insulated wire under

wet condition. IEEJ Trans PE 2014;134(5):419–426 (in Japanese); Electrical Engineering in Japan 2016;194(4):1–9 (in English).

14. Arai K, Sano K, Tsunoda Y. Impulse corona discharge from water drops on a cylindrical conductor. T IEE Japan 1972;92(1):39–48. (in Japanese)

AUTHORS (from left to right)




Toshiyuki Nishi (member) was born on March 8, 1959. In March 1983, Nishi completed the Master's program at Graduate School of Engineering, Kanazawa University. He joined USAC Electronic Industrial (now, PFU Ltd.) in April 1983. He became Research Associate at the Department of Electrical Engineering, Toyama National College of Technology (now, Department of Electrical and Control Systems Engineering, National Institute of Technology, Toyama College) in April 1985, promoted as a Lecturer in July 1993, and as an Assistant Professor in April 1997. Since April 2006, he has been a Professor. He is engaged in studies related to creeping discharge phenomena. He is a Doctor of Engineering.

Ryoichi Hanaoka (member) was born on January 12, 1950. In March 1980, Hanaoka completed the Master's program at Graduate School of Engineering, Kanazawa University. He became Lecturer at Kanazawa Institute of Technology in April 1988, an Assistant Professor in 1989, and has been a Professor since 1996. He is engaged in studies related to electric conductivity and dielectric breakdown in liquid dielectrics, and electric field calculation methods. From September 1993 to August 1994, he was a Guest Researcher at MIT (USA). He is a Doctor of Engineering. He has a membership of IESJ and IEEE.

Fri Murdiya (nonmember) was born on February 5, 1980. In 2009, Murdiya completed the Master's program at Graduate School of Engineering, Institut Teknologi Bandung (Indonesia). He became Lecturer at the University of Riau in April 2010. Since September 2014, he has been attending the doctoral program at Graduate School of Engineering, Kanazawa Institute of Technology. He is engaged in research on lightning protection systems and creeping discharge phenomena in cables and liquid dielectrics.

Katsunori Miyagi (senior member) was born on February 11, 1957. In March 1980, Miyagi graduated from the Department of Electrical Engineering, Division of Engineering, Muroran Institute of Technology. He completed the Master's program at Department of Electrical Engineering, Graduate School of Engineering, Muroran Institute of Technology in March 1982. He joined Meidensha Corporation in April 1982 and then Japan AE Power Systems in October 2002. Since April 2012, he has been a Professor at Kanazawa Institute of Technology. He is mainly engaged in insulation technologies for power devices and high voltage measurement. He is a Doctor of Engineering. He is a President of National Committee IEC TC10 (Fluids for Electrotechnical Applications). He received 2007 IEEJ Best English Paper Award. He has a membership of IEEE and CIGRE.